First Observation of the Decay $D_s^+ \to p\bar{n}$

S. B. Athar,[1] R. Patel,[1] J. Yelton,[1] P. Rubin,[2] B. I. Eisenstein,[3] I. Karliner,[3] S. Mehrabyan,[3] N. Lowrey,[3] M. Selen,[3] E. J. White,[3] J. Wiss,[3] R. E. Mitchell,[4] M. R. Shepherd,[4] D. Besson,[5] T. K. Pedlar,[6] D. Cronin-Hennessy,[7] K. Y. Gao,[7] J. Hietala,[7] Y. Kubota,[7] T. Klein,[7] B. W. Lang,[7] R. Poling,[7] A. W. Scott,[7] P. Zweber,[7] S. Dobbs,[8] Z. Metreveli,[8] K. K. Seth,[8] A. Tomaradze,[8] J. Libby,[9] A. Powell,[9] G. Wilkinson,[9] K. M. Ecklund,[10] W. Love,[11] V. Savinov,[11] A. Lopez,[12] H. Mendez,[12] J. Ramirez,[12] J. Y. Ge,[13] D. H. Miller,[13] I. P. J. Shipsey,[13] B. Xin,[13] G. S. Adams,[14] M. Anderson,[14] J. P. Cummings,[14] I. Danko,[14] D. Hu,[14] B. Moziak,[14] J. Napolitano,[14] Q. He,[15] J. Insler,[15] H. Muramatsu,[15] C. S. Park,[15] E. H. Thorndike,[15] F. Yang,[15] M. Artuso,[16] S. Blusk,[16] S. Khalil,[16] J. Li,[16] R. Mountain,[16] S. Nisar,[16] K. Randrianarivony,[16] N. Sultana,[16] T. Skwarnicki,[16] S. Stone,[16] J. C. Wang,[16] L. M. Zhang,[16] G. Bonvicini,[17] D. Cinabro,[17] M. Dubrovin,[17] A. Lincoln,[17] P. Naik,[18] J. Rademacker,[18] D. M. Asner,[19] K. W. Edwards,[19] J. Reed,[19] R. A. Briere,[20] T. Ferguson,[20] G. Tatishvili,[20] H. Vogel,[20] M. E. Watkins,[20] J. L. Rosner,[21] J. P. Alexander,[22] D. G. Cassel,[22] J. E. Duboscq,[22] R. Ehrlich,[22] L. Fields,[22] L. Gibbons,[22] R. Gray,[22] S. W. Gray,[22] D. L. Hartill,[22] B. K. Heltsley,[22] D. Hertz,[22] J. M. Hunt,[22] J. Kandaswamy,[22] D. L. Kreinick,[22] V. E. Kuznetsov,[22] J. Ledoux,[22] H. Mahlke-Krüger,[22] D. Mohapatra,[22] P. U. E. Onyisi,[22] J. R. Patterson,[22] D. Peterson,[22] D. Riley,[22] A. Ryd,[22] A. J. Sadoff,[22] X. Shi,[22] S. Stroiney,[22] W. M. Sun,[22] and T. Wilksen[22]

(CLEO Collaboration)

[1]*University of Florida, Gainesville, Florida 32611, USA*
[2]*George Mason University, Fairfax, Virginia 22030, USA*
[3]*University of Illinois, Urbana-Champaign, Illinois 61801, USA*
[4]*Indiana University, Bloomington, Indiana 47405, USA*
[5]*University of Kansas, Lawrence, Kansas 66045, USA*
[6]*Luther College, Decorah, Iowa 52101, USA*
[7]*University of Minnesota, Minneapolis, Minnesota 55455, USA*
[8]*Northwestern University, Evanston, Illinois 60208, USA*
[9]*University of Oxford, Oxford OX1 3RH, United Kingdom*
[10]*State University of New York at Buffalo, Buffalo, New York 14260, USA*
[11]*University of Pittsburgh, Pittsburgh, Pennsylvania 15260, USA*
[12]*University of Puerto Rico, Mayaguez, Puerto Rico 00681*
[13]*Purdue University, West Lafayette, Indiana 47907, USA*
[14]*Rensselaer Polytechnic Institute, Troy, New York 12180, USA*
[15]*University of Rochester, Rochester, New York 14627, USA*
[16]*Syracuse University, Syracuse, New York 13244, USA*
[17]*Wayne State University, Detroit, Michigan 48202, USA*
[18]*University of Bristol, Bristol BS8 1TL, United Kingdom*
[19]*Carleton University, Ottawa, Ontario, Canada K1S 5B6*
[20]*Carnegie Mellon University, Pittsburgh, Pennsylvania 15213, USA*
[21]*Enrico Fermi Institute, University of Chicago, Chicago, Illinois 60637, USA*
[22]*Cornell University, Ithaca, New York 14853, USA*

(Received 7 March 2008; published 7 May 2008)

Using $e^+e^- \to D_s^{*-}D_s^+$ data collected near the peak D_s production energy, $E_{\rm cm} = 4170$ MeV, with the CLEO-c detector, we present the first observation of the decay $D_s^+ \to p\bar{n}$. We measure a branching fraction $\mathcal{B}(D_s^+ \to p\bar{n}) = (1.30 \pm 0.36^{+0.12}_{-0.16}) \times 10^{-3}$. This is the first observation of a charmed meson decaying into a baryon-antibaryon final state.

DOI: 10.1103/PhysRevLett.100.181802 PACS numbers: 13.25.Ft

Of the three ground-state charmed mesons, only the D_s^+ is massive enough to decay to a baryon-antibaryon pair. Even before the discovery of the D_s^+, a search for the decay $D_s^+ \to p\bar{n}$ was suggested [1] as a "smoking gun" for decays proceeding via annihilation through a virtual W^+, and a prediction was made that the branching fraction would be $\approx 1\%$ if the annihilation mechanism dominated D_s^+ decays. In the intervening period it has become clear that the annihilation diagram contributes to, but does not dominate, D_s^+ decays, and has been studied in purely leptonic decays such as $D_s^+ \to \mu\nu$ [2] and $D_s^+ \to \tau\nu$ [3]. However, although the theoretical study of $D_s^+ \to p\bar{n}$ is complicated by final state interactions, it still has a unique role to play in the understanding of charmed meson decays.

Finding decay modes that include an (anti-)neutron is particularly challenging. CLEO-c is the first detector to have a large dataset (≈ 325 pb^{-1}) of e^+e^- annihilation events taken at a center-of-mass energy of around 4170 MeV. At this energy, there is a substantial cross section (≈ 1 nb) for the reaction $e^+e^- \to D_s^{*-}D_s^+$ [4]. Using the knowledge of center-of-mass energy and momentum, we use a missing-mass method to find the (anti-)neutron and so do not depend upon its interaction in the detector. Therefore, in this Letter, mention of a particular decay mode implies the use of the charge conjugate decay mode also.

The CLEO-c detector [5] is designed to measure the momenta of charged particles which curve in a 1.0 T solenoidal magnetic field, and identify them using specific energy loss (dE/dx) and Cherenkov imaging (RICH). Photons are detected, and their energy measured, using a CsI calorimeter. Our analysis procedure has much in common with that used in the measurement of $\mathcal{B}(D_s^+ \to \mu\nu)$ [2]. Here, we fully reconstruct one D_s^- as a "tag," reconstruct a transition photon from a D_s^* decay, and identify and measure the momentum of a proton. We can then reconstruct the missing mass of the event and look for a peak at the antineutron mass.

The D_s^- tags are found in the eight modes: $K^+K^-\pi^-$, $K_s^0K^-$, $\eta\pi^-$, $\eta'\pi^-$, $\phi\rho^-$, $\pi^-\pi^+\pi^-$, $K^{*-}K^{*0}$ and $\eta\rho^-$. Track selection, particle identification, and definition of resonances are similar to those in our previous publication [2], with one important exception; each of the charged tracks in the D_s^- tag is required to have a dE/dx measurement more than 3 standard deviations, σ, away from that expected for a proton. All the D_s^- tags are required to have momentum consistent with coming from the two-body production $D_s^*D_s$. Figure 1 shows the measured mass of the tag candidate minus the nominal D_s^- mass, divided by the resolution of the candidate tag's mode. The fit shown is a unit Gaussian centered at zero. Those candidates within 2.5 of the peak are kept as D_s^- tags. According to the fit they comprise 27 700 real D_s^- mesons and 64 900 background combinations. Those combinations in the regions $\pm(3.5-6.0)$ in this plot will be used as a check on the combinatorial background to our final signal. We kinematically constrain the mass of the tags in the signal region to the known mass of the D_s^-. To be consistent, each sideband tag is kinematically constrained to the center of its sideband.

We now add a γ that satisfies our shower shape requirements to the D_s^- tag. Using the four-momenta of the γ candidate, $p(\gamma)$, and the D_s^- tag, we calculate the four-momentum of the D_s^+ using the equation $p(D_s^+) = p_{\rm beam} - p(D_s^-) - p(\gamma)$. The four-momentum of the beam, $p_{\rm beam}$ takes into account the small crossing angle of the CESR beams. The missing-mass squared (MM^2) distribution for good tag events is shown in Fig. 2. It shows a peak at $M^2(D_s^+)$ corresponding to $D_s^*D_s$ production. This is fit to a signal shape of a Crystal Ball function [6] with fixed tail parameters derived from Monte Carlo simulation, together with a fifth order polynomial background function. We select those events with MM^2 values between

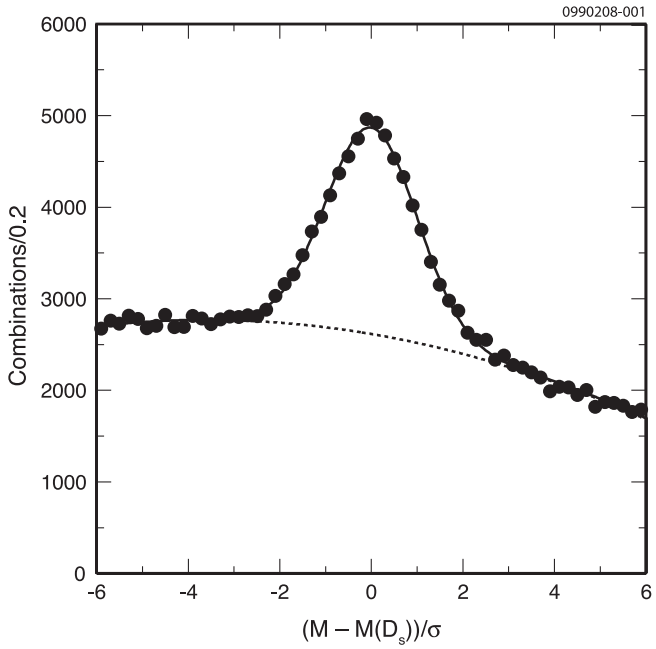

FIG. 1. The reconstructed mass minus the known D_s mass, divided by the detector resolution, for all eight modes of D_s tags reconstructed. The fit shown is a unit Gaussian centered at zero, together with a second order polynomial background function.

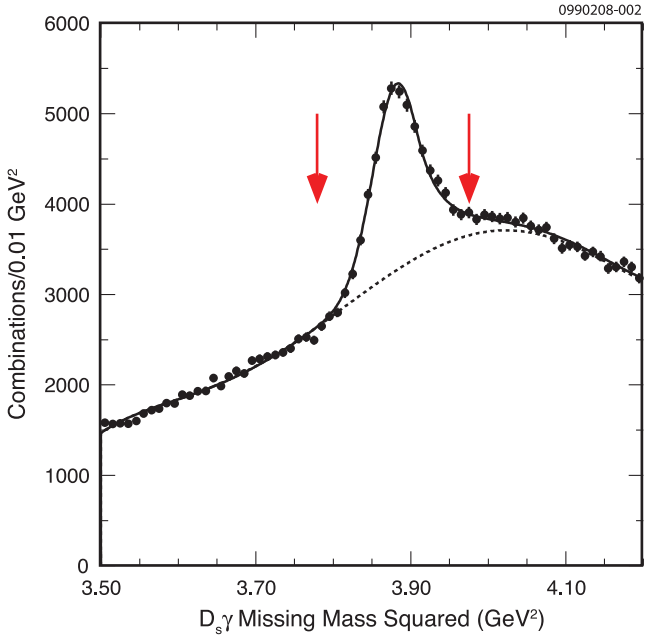

FIG. 2 (color online). The missing-mass squared from events with a reconstructed γ and D_s(tag). The fit is to a signal shape of a Crystal Ball function [6] with fixed tail parameters, together with a fifth order polynomial background function.

3.779 and 3.976 GeV^2. This is a loose requirement, with most of the loss in efficiency due to initial state radiation of the beam, which smears the MM^2 to artificially high values. According to the fit, the yield of $D_s^- \gamma D_s^+$ candidates in this range is 16 955 above a background of 63 170. This yield will be the denominator in our final branching fraction calculation.

We next select our proton candidate. Monte Carlo simulation shows that all protons from this decay mode will have momenta in the range 150–550 MeV/c. This is below the momentum range for the RICH detector to identify protons, but well suited to identification by dE/dx. We require that this measurement be within 3σ of that expected for a proton, and greater than 3σ from that expected for a kaon or a pion. The overall proton efficiency is determined by Monte Carlo simulation to be 75%, with the efficiency lowest at the lower proton momenta.

We may now calculate the missing 4-momentum in the event, equal to the expression $p_{\text{beam}} - p(D_s^-) - p(\gamma) - p_{\text{proton}}$, and can thus calculate the missing mass of the event. However, we have further kinematic constraints we can impose which allow us to improve the missing-mass resolution and reject combinatorial background. We do not know *a priori* if the photon is due to the transition $D_s^{*-} \to D_s^-(\text{tag})\gamma$, or $D_s^{*+} \to D_s^+(\text{signal})\gamma$. We perform kinematic fits with each assumption, and choose between the two based on the χ^2 values of the two fits. First, we add the photon to the D_s^- tag to form a D_s^{*-} candidate, and constrain the momentum of this D_s^{*-} candidate to that calculated from the two-body production $e^+e^- \to D_s^{*-}D_s^+$. We then constrain the mass difference $M(D_s^{*-}) - M(D_s^-)$ to its nominal value. Alternatively, we constrain the D_s^- tag itself to the momentum calculated assuming the two-body production $e^+e^- \to D_s^- D_s^{*+}$, then combine the proton with the missing mass of the event to make a D_s signal candidate, add the photon, and constrain the $M(D_s^{*+} - D_s^+)$ mass difference. We choose the scheme with the lowest total χ^2 value; in Monte Carlo simulation we find that we assign the photon to the correct D_s greater than 95% of the time. The kinematic constraints on the detected particles improve the resolution in missing mass by around a factor of 2, whichever D_s the photon is combined with. Furthermore, we can place cuts on the χ^2 of the kinematic constraints to reject combinatorial background. In the case of the momentum constraint we require $\chi^2 < 9$, and in the case of the mass-difference constraint we require $\chi^2 < 4$; with each constraint there is 1 degree of freedom. The requirement is looser for the momentum constraint because initial state radiation produces a tail in the momentum distribution.

The transition photon in the event has an energy in the laboratory of 110–180 MeV. In this energy range there is the possibility of background clusters passing all the requirements for being a photon. Such background photons are particularly prevalent in events which contain antibaryons as they frequently interact with the detector and give "split-off" clusters, often far from the impact point of the particle in the CsI calorimeter. Occasionally an event may survive all the above requirements while having more than one photon candidate. If so, we select the photon candidate that produces the lowest combined χ^2 in the kinematic fit. Background photons also influence the signal shape which we determine using Monte Carlo simulation. This shape is well described by a core Gaussian function of $\sigma \approx 4$ MeV centered at the neutron mass, together with a second, offset, Gaussian of width $\sigma \approx 38$ MeV and containing $\approx 12\%$ of the signal. This second Gaussian is due to events where we have used an incorrect photon candidate.

Figure 3 shows the missing-mass distribution for the events after all requirements and kinematic fitting, and contains 13 events. These are the only events in the missing-mass range 600–1100 MeV. The plot is well fit using a likelihood fit to the signal shape described above, so we take our signal yield to be the 13.0 ± 3.6 events observed. Repeating the analysis using sidebands to the D_s^- as described above, gives three events in the missing-mass range 600–1100 MeV, none of which are in the signal region of 900–980 MeV. We divide this yield of 13 by the number of D_s^+ decays we have detected, and correct for the efficiencies of requirements placed on the fit χ^2 and proton reconstruction and identification. This gives a branching fraction of $(1.30 \pm 0.36) \times 10^{-3}$, where the error shown is the statistical error in the signal yield only.

We have performed many checks to ensure that our analysis is not biased towards obtaining events only in

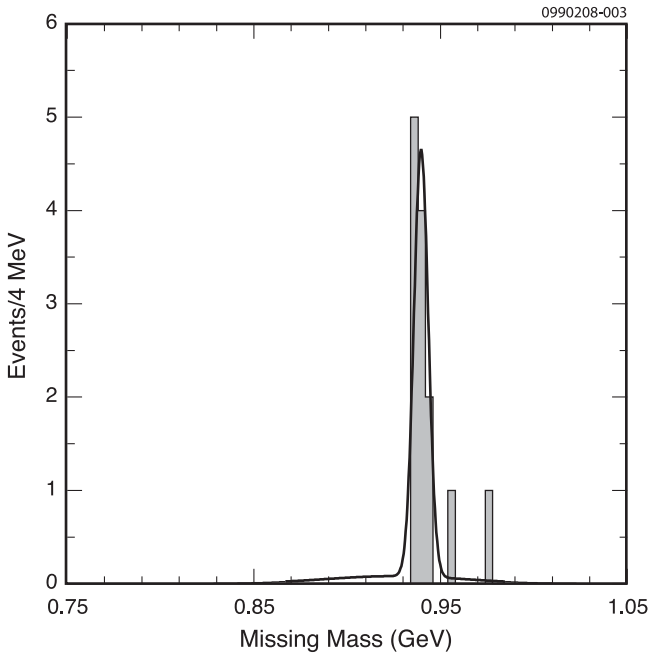

FIG. 3. The missing mass in the event after all requirements and kinematic fitting has been performed. The fit is described in the text.

the signal region. To enter the final signal plot, an event must have a proton candidate of a momentum which happens to be well matched to the capabilities of the dE/dx system, and thus background from incorrectly identified proton candidates is negligible. This, in turn, means that background from other charm events is negligible. In order to check that the sidebands are a reasonable representation of combinatorial background, we generated a large sample of *uds* continuum Monte Carlo events with final states of a proton, an antineutron, a photon, and the decay products of a D_s^-. Very few of these events passed all the kinematic requirements, and among those that did, there were as many antineutron candidates in the sideband plot as the signal plot.

As a check on the efficiency of the selection criteria imposed on the quality of the kinematic fit, we repeated the analysis looking for the decay $D_s^+ \to K^+ K^0$, where we consider the K^0 to be the missing-mass analog of the antineutron. We reproduce very well the measurement of this branching fraction found by more direct means [7], and from the comparison of the efficiencies of the kinematic constraint cuts in data and Monte Carlo calculations, we find a systematic uncertainty in the efficiency of $\pm 4\%$. The uncertainty in the number of D_s^+, the denominator in our branching fraction calculation, is systematically limited, and by looking at the variation of the yield using a variety of different signal and background functions, estimated to be $\pm 5\%$. One possible source of systematic uncertainty concerns the signal shape, the tail of which is dominated by split offs from antibaryon interactions which are one of the hardest processes to reliably simulate. We conservatively assign a $\pm 6\%$ uncertainty to account for any mismodeling of this process; this number corresponds to getting the number of events from these fake photons incorrect by $\pm 50\%$. Last, we note that although there is no evidence of any background in the final plot, we cannot assume that it is strictly zero. As our best estimate of the background is 0 events, which corresponds to an upper limit (1σ) of 1.1 events, we therefore introduce a -8.5% uncertainty in the final branching fractions. Combining these systematic uncertainties in quadrature, produces a total systematic uncertainty of $^{+9}_{-12}\%$ in the branching fraction, much smaller than the statistical error.

In conclusion, we report the first observation of the decay $D_s^+ \to p\bar{n}$ with a signal of 13 events and a background consistent with zero. We measure the branching fraction $\mathcal{B}(D_s^+ \to p\bar{n}) = (1.30 \pm 0.36^{+0.12}_{-0.16}) \times 10^{-3}$. This is the first observation of a charm meson decaying into baryon-antibaryon pair. The two-body decay observed here is the only one allowed kinematically. The actual decay process is suspected to be related to annihilation, which is also responsible for purely leptonic decays. Relating this baryonic decay rate to the leptonic rate should provide important clues as to how baryons are produced in hadronic interactions.

We gratefully acknowledge the effort of the CESR staff in providing us with excellent luminosity and running conditions. This work is supported by the A. P. Sloan Foundation, the National Science Foundation, the U.S. Department of Energy, the Natural Sciences and Engineering Research Council of Canada, and the U.K. Science and Technology Facilities Council.

[1] Xuan Yem Pham, Phys. Rev. Lett. **45**, 1663 (1980).
[2] M. Artuso *et al.* (CLEO Collaboration), Phys. Rev. Lett. **99**, 071802 (2007); T. Pedlar *et al.* (CLEO Collaboration), Phys. Rev. D **76**, 072002 (2007).
[3] K. M. Ecklund *et al.* (CLEO Collaboration), Phys. Rev. Lett. **100**, 161801 (2008).
[4] D. Cronin-Hennessy *et al.* (CLEO Collaboration), arXiv:0801.3418 [Phys. Rev. D (to be published)].
[5] Y. Kubota *et al.* (CLEO Collaboration), Nucl. Instrum. Methods Phys. Res., Sect. A **320**, 66 (1992); D. Peterson *et al.*, Nucl. Instrum. Methods Phys. Res., Sect. A **478**, 142 (2002); R. A. Briere *et al.* (CESR-c and CLEO-c Taskforces, CLEO-c Collaboration), Cornell University, LEPP Report No. CLNS 01/1742 2001 (unpublished).
[6] P. Rubin *et al.* (CLEO Collaboration), Phys. Rev. D **73**, 112005 (2006).
[7] J. Alexander *et al.* (CLEO Collaboration), Phys. Rev. Lett. **100**, 161804 (2008).